

# Hydrogenation of Citral over Ni and Ni-Sn Catalysts

Hilal AYKAÇ, Selahattin YILMAZ\*

*İzmir Institute of Technology, Chemical Engineering Department,  
Gülbağçe Köyü, Urla, İzmir-TURKEY  
e-mail: selahattinyilmaz@iyte.edu.tr*

Received 26.03.2007

Liquid phase citral hydrogenation over zeolite-supported monometallic Ni and bimetallic Ni-Sn catalysts was studied. The zeolite support materials were Na-Y, Na-mordenite, and clinoptilolite. Ni and Sn contents of the monometallic and bimetallic catalysts were 8.1-9.2 wt% and 0.46 wt%, respectively. The type of the zeolite support affected the activity and selectivity of the catalysts differently. The main product of the citral hydrogenation reaction was citronellal, for both monometallic (84.5% yield) and bimetallic (44.5% yield) catalysts. The addition of promoter increased the selectivity to unsaturated alcohols (geraniol+nerol), i.e. it changed from 0.9% to 6.3% over mordenite and from 0.9% to 2.1% over Na-Y-supported catalysts. Furthermore, activity of the Ni catalysts decreased while the quantity of acetal remained almost constant. Intimate contact between active metal, promoter, and support, and a catalyst with a high concentration of weak acid sites gave high selectivity to geraniol+nerol.

**Key Words:** Citral, hydrogenation, citronellol, Ni, Ni-Sn, zeolite.

## Introduction

Selective hydrogenation of  $\alpha - \beta$  unsaturated aldehydes is a difficult challenge in the organic synthesis of fine chemicals because the C=C bond is attacked much more easily than the C=O bond when a conventional heterogeneous catalyst is used.<sup>1</sup>

Citral hydrogenation is a complex reaction: there are series and parallel reactions. Products formed over different catalysts include citronellal, citronellol, geraniol, nerol, 3, 7 dimethyl alcohol, menthol, isopulegol, citral and citronellal acetals, and unidentified products. Unsaturated alcohols (geraniol, nerol, and citronellol) are desired products. Geraniol and nerol are formed by the selective hydrogenation of the citral carbonyl group.<sup>2,3</sup> The citral hydrogenation reaction scheme is given in Figure 1.

Many attempts have been made to develop heterogeneous catalysts suitable for this reaction. For this purpose, noble metals (Pt, Ni, Ru, Rh, and Pd) supported on several synthetic and natural zeolites were used as heterogeneous catalysts. The performance of the supported noble metals for the selective hydrogenation of the C=O bond were enhanced by combining them with promoters (Sn, Ge, Fe).<sup>1,4</sup> Supported Ni catalysts have been investigated extensively<sup>5</sup> and have shown some selectivity to unsaturated alcohols. The addition of tin has been shown to improve their performance and selectivity.<sup>6,7</sup>

---

\*Corresponding author

Zeolite supports introduce the possibility of metal-support interactions; active metal properties can be polarized by nearby cations or by metal-support interaction.<sup>8</sup> Recently, zeolite-supported catalysts were tested in the hydrogenation of citral.<sup>9</sup> Maki-Arvela et al. studied the activity and selectivity of Ni on H and the NH<sub>4</sub> form of the zeolite Y in citral hydrogenation.<sup>5</sup> These catalysts gave low selectivity to desired products. Instead, cracking, cyclization, and dehydrogenation reactions took place, because of the acidic property of the catalyst. In our previous study, Pd-loaded clinoptilolite-rich natural zeolite was used as a support material. The catalyst was highly selective to citronellal.<sup>10</sup> The addition of Sn has been reported to increase the selectivity of active metals to unsaturated alcohols;<sup>7,11–13</sup> however, in some studies the addition of Sn decreased the activity of the catalyst while the selectivity to unsaturated alcohols increased.<sup>13,14</sup>

The purpose of the present investigation was to prepare active and selective zeolite-supported monometallic (Ni) and bimetallic (Ni-Sn) catalysts for the selective hydrogenation of citral in order to produce unsaturated alcohols, namely nerol, geraniol, and citronellol. Catalysts were prepared by impregnation and co-impregnation methods. The zeolite support materials were Na-Y, Na-mordenite (Mor), and clinoptilolite (Clino).

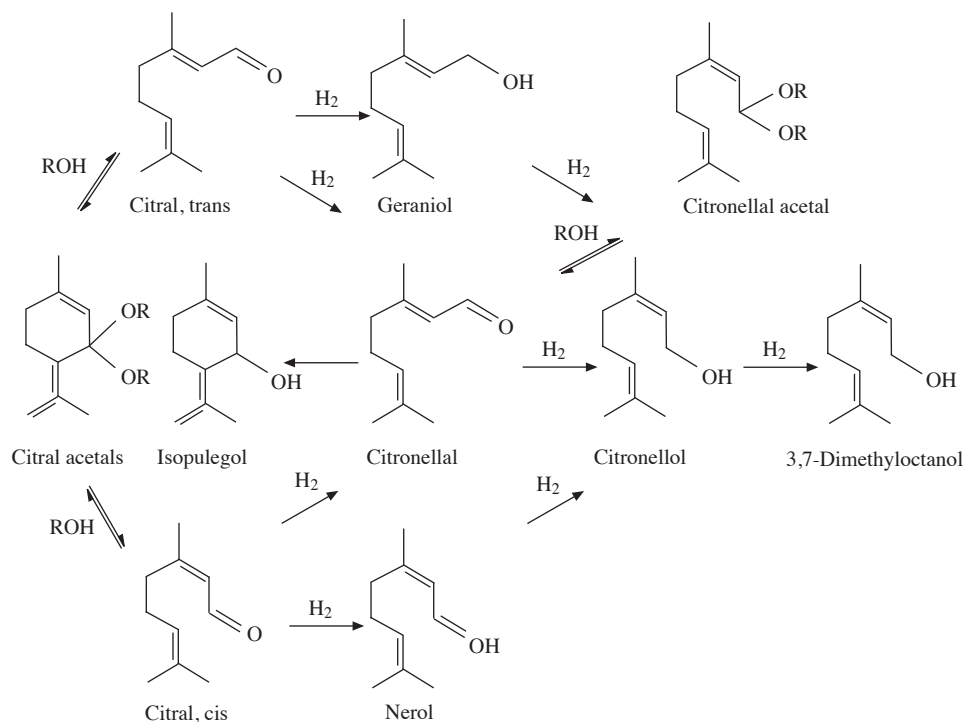


Figure 1. Reaction scheme for citral hydrogenation.<sup>5</sup>

## Experimental

### Preparation of Catalysts

Na-Mor (Süd-Chemie, MOR powder) and Na-Y (Zeolyst, CBV100 powder) were obtained commercially. Clino-rich natural zeolite chunks (Gördes, Manisa, Turkey) were crushed and sieved to the desired particle size range (38–150 μm). Clino samples were washed and dried prior to calcination. The zeolites were calcined at 500 °C under an N<sub>2</sub> flow (100 mL/min) for 5 h in a tubular reactor and then used as catalyst supports.

Monometallic Ni catalysts were prepared by the impregnation method. The supports were contacted with an ethanol solution of 0.01 M  $\text{Ni}(\text{NO}_3)_2 \cdot 6\text{H}_2\text{O}$  for 16 h with a magnetic stirrer at room temperature. Then, ethanol was evaporated in a rotary evaporator at 45 °C for 1 h. The impregnated supports were dried overnight in an oven at 120 °C and then calcined at 500 °C under a dry air flow (100 mL/min) for 5 h. Bimetallic catalysts (Ni-Sn) were prepared by the co-impregnation method. An ethanol solution of  $\text{Ni}(\text{NO}_3)_2 \cdot 6\text{H}_2\text{O}$  and  $\text{SnCl}_2 \cdot 2\text{H}_2\text{O}$  was used. Ni loading of the catalysts was kept constant as monometallic catalysts. The Sn/(Sn+Ni) mole ratio was 0.02 for all of the catalysts, which were calcined as monometallic catalysts.

## Characterization of the Catalysts

The prepared catalysts were characterized using different instrumental techniques, namely scanning electron microscopy (Philips SFEG 30S SEM), elemental analysis (Varian Liberty II ICP-AES), X-ray diffraction (Philips X'Pert Pro with Cu  $K\alpha$  radiation), and nitrogen adsorption (Micromeritics, ASAP 2010).

Acidity of the samples was determined by the temperature-programmed desorption of ammonia ( $\text{NH}_3$ -TPD) method using a Micromeritics AutoChem II chemisorption analyzer. The sample was heated to 500 °C at the rate of 5 °C/min and kept at this temperature for 1 h under a He gas flow of 70 mL/min. Then, the sample was cooled under a He flow of 30 mL/min to 90 °C at the rate of 5 °C/min. This was followed by switching the flow to a  $\text{NH}_3$ -He gas mixture at the rate of 30 mL/min for 30 min. Physically adsorbed  $\text{NH}_3$  was removed by degassing the sample at 90 °C under a He flow of 70 mL/min for 120 min and then at a rate of 30 mL/min for 150 min.  $\text{NH}_3$  desorption of the sample was analyzed by heating the sample at a rate of 10 °C/min, from 90 °C to 600 °C. The TCD signal was recorded during the  $\text{NH}_3$ -TPD.

Temperature-programmed reduction (TPR) and temperature-programmed desorption of  $\text{H}_2$  ( $\text{H}_2$ -TPD) were carried out using the same apparatus as used for  $\text{NH}_3$ -TPD measurements. The catalyst samples were outgassed at 500 °C for 1 h and then cooled to 50 °C under a He flow. TPR profiles were registered by heating the samples from room temperature to 600 °C at the rate of 5 °C/min under a flow of 5%  $\text{H}_2$ /He mixture (20 mL/min). The flow was then switched to He and the samples were cooled to 50 °C. For  $\text{H}_2$ -TPD they were heated to 600 °C under a He flow (30 mL/min).

## Catalyst Testing

Citral (mixture of cis- and trans-isomers, Fluka, purity 97%,) hydrogenation experiments were performed in a stirred semi-batch reactor (model 4574, Parr Instrument Co.). Before the reaction the catalysts (250 mg) were reduced in situ under a  $\text{H}_2$  flow (80-100 mL/min) for 2 h under 4 bar at 400 °C. Then, the reactor was cooled to reaction temperature. Reactant mixture (200 mL of 0.1 M citral in ethanol) was injected into the bubbling unit to remove the dissolved oxygen before it was injected into the reactor and contacted with the catalysts. Citral was hydrogenated at 80 °C under 6 bar  $\text{H}_2$  with a stirring rate of 600 rpm. The liquid samples were withdrawn from the reactor at known time intervals. Preliminary tests showed that the reaction was kinetically controlled under the condition studied.

Samples taken from the reactor were analyzed with an Agilent Technologies 6890N Network GC System gas chromatograph equipped with a flame ionization detector and a DB-225 capillary column (J&W, 30 m, 0.53 mm ID). Hydrogenation products of citral were identified by the GC-MS technique (Varian Saturn 2000). The composition of components in the reaction mixture was determined by the internal standardization method.

## Results and Discussion

### Catalyst Characterization

The physicochemical and textural properties of the catalyst supports are given in Table 1. Aluminum content of the supports decreased in the following order: Na-Y > Clino > Na-Mor. As Si/Al ratios were low, these supports were expected to have high concentrations of acid sites with low strength.

**Table 1.** Physicochemical and textural properties of the supports.

Catalyst Supports	Si/Al	$S_{BET}$ (m <sup>2</sup> /g)	* $V_p$ (cm <sup>3</sup> /g)	Active Metal Mean particle size (nm)
Na-Y	2.6	886.1	0.463	-
Ni/Na-Y	2.6	785.7	0.404	11.8
Ni-Sn/Na-Y	2.6	704.2	0.360	11.7
Na-Mor	9.0	406	0.217	-
Ni/Na-Mor	9.0	394.8	0.209	14.2
Ni-Sn/Na-Mor	9.0	363.3	0.176	15.9
Clino	5.3	43.3	0.065	-
Ni/Clino	5.3	38.7	0.081	12.1

\* $V_p$ : Micropore volume.

Ni content of the catalysts ranged between 8.1 and 9.2 wt%. The bimetallic catalyst Sn/(Ni+Sn) mol ratio was 0.02, which gave 0.46 wt% Sn.

It was observed that the catalyst had large surface areas, except the Clino-supported catalysts. As Clino had the lowest pore size among the supports studied, only the surface area of the pores that were accessible by N<sub>2</sub> molecules were measured. The surface areas and pore volumes decreased as metal loading increased. This could have been due to the blockage and/or narrowing of some of the pores due to metal loading. The shape of the adsorption isotherms remained the same as metal loading increased. This also confirmed that the crystal structure was preserved after loading. Surface area of the catalysts reduced more when bimetallic catalysts were prepared and reduction of up to 10% was observed. This could have been due to partial pore blocking and/or pore narrowing.

SEM micrographs of the supports show that the morphologies of the samples were different. Clino, Na-Mor and Na-Y had large and more distinct crystallites. The size of the crystallites of these supports ranked as follows: Clino (~7 μm) > Na-Y (~400 nm) > Na-Mor (~150 nm).

XRD patterns of the different supports used and catalysts prepared are given in Figure 2. The characteristic peaks of each support were observed in XRD patterns of all monometallic and bimetallic catalysts. This showed that the crystallinity of the support was preserved during catalyst preparation. Ni peaks were observed at  $2\theta$  of 37.3° and 43.3° for all of the catalysts. Since Sn content of the catalysts was low, the Sn peak could not be observed by XRD. The peak of the nickel-tin alloy (Ni<sub>3</sub>Sn<sub>2</sub>) was also observed at  $2\theta$  of 30.3° and 43.7° for Na-Y and Na-Mor supported bimetallic catalysts. Mean active metal particle sizes, calculated using the Scherrer equation by analysis of the nickel peak at  $2\theta$  of 43.7°, are given in Table 1. These results suggest that at least part of the metal was at the outer surface of the support.

Larger particles formed on Na-Mor, as it had the smallest surface area among the catalysts prepared.

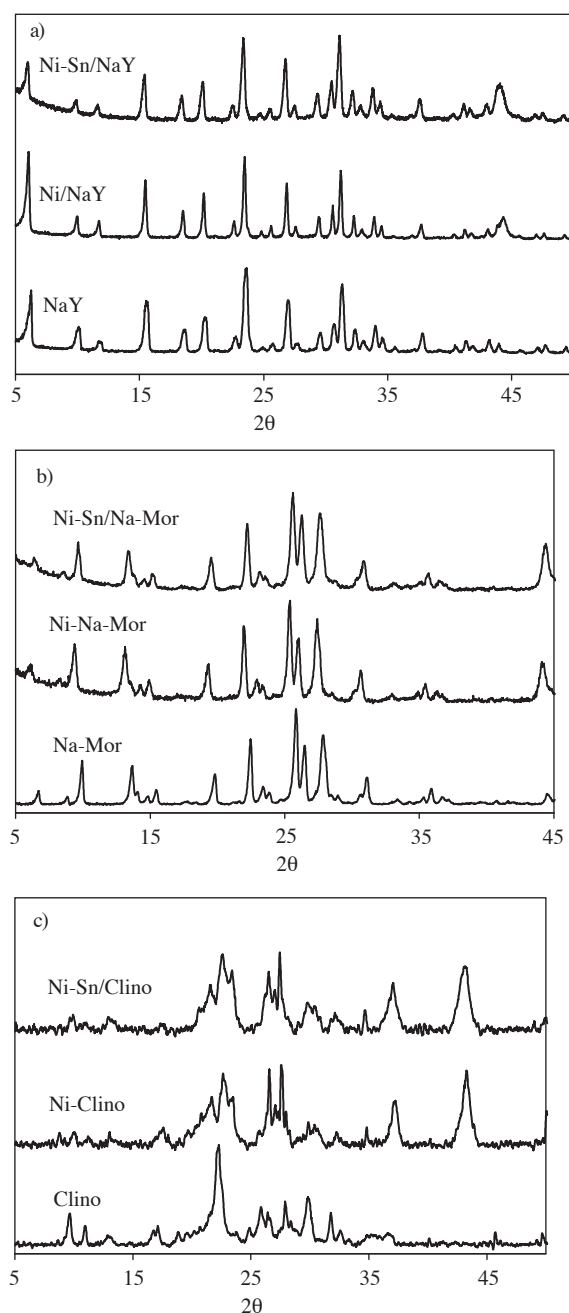


**Figure 2.** XRD patterns of the different supports and catalysts.; a) Na-Y and Na-Y-supported catalysts; b) Na-Mor and Na-Mor-supported catalysts; c) Clino and Clino-supported catalysts.

Acidity of each catalyst is given in Figure 3. Findings show that the addition of Sn decreased the number of acid sites in Ni/Na-Mor and Ni/Na-Y. With Na-Mor, the concentration of high strength acid sites (desorption temperature  $> 300$  °C) were reduced, while with Na-Y the concentration of weak and strong acid sites were reduced. Using a Cl precursor did not increase the catalysts acidity. Among the monometallic and bimetallic catalysts, those that were Na-Mor-supported had the highest acidity.

H<sub>2</sub>-TPD showed that the temperature at the maximum peaks was 286 and 304 °C for Ni-Sn/Na-Mor and Ni-Sn/Na-Mor, respectively; however, there was a significant difference in the TPR of these samples. The reduction of Ni-Sn/Na-Mor started at 120 °C and reached 380 °C, giving a maximum peak at 254 °C, but reduction of Ni-Sn/Na-Y started at 372 °C, continued up to 514 °C, and exhibited a peak maximum around 496 °C. This shows that there were different metal support interactions and that metal support interaction was higher over the Na-Y zeolite. The interaction could differ as 2 supports have different surface areas and morphologies. Such interaction could dramatically change the crystallography and the electronic state of the metal particles.<sup>15</sup> The lower reduction temperature of Ni-Sn/Na-Mor indicates intimate contact between the 2 metals in the bimetallic catalyst. As a result, higher selectivity over this catalyst was obtained. In addition, acid site concentration of Ni-Sn/Na-Mor was higher than that of Ni-Sn/Na-Y. As no cracking or isomerization reactions were observed, it is suggested that the acid sites were mainly of the Lewis acid-type. Lewis acid-types have been reported to increase selectivity to unsaturated alcohols.<sup>16</sup>

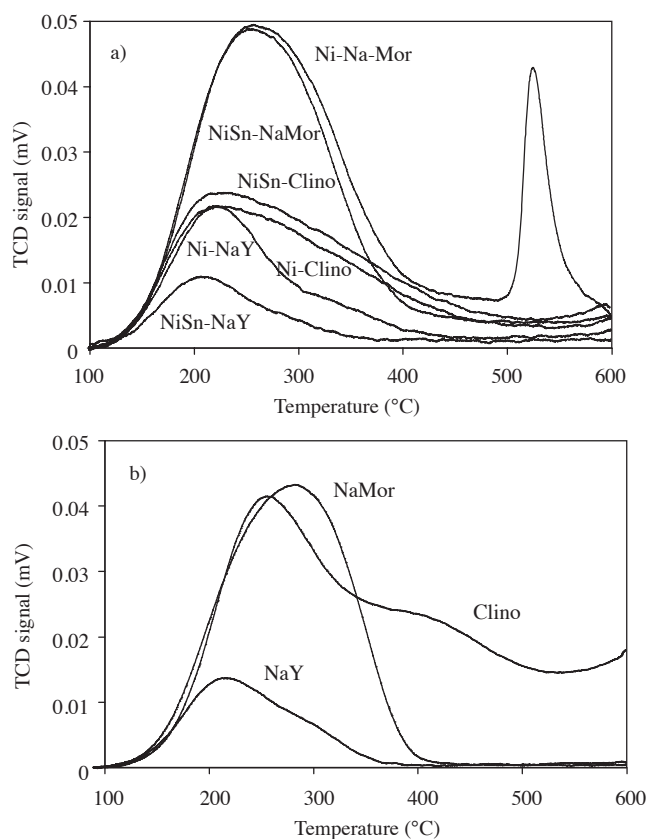


**Figure 3.** NH<sub>3</sub>-TPD of the catalysts (a) and the supports (b).

## Catalyst Testing

The product distribution over Ni/Na-Y is given as an example in Figure 4. The quantity of citral decreased quite sharply at the beginning of the reaction. Then, the quantity of citral decreased with time until conversion was almost complete. Citronellal, citronellol, geraniol, isopulegol, acetals (citral+citronellal acetals), and some unidentified products were formed. The major product was citronellal, which increased in quantity as the reaction proceeded (84.5% yield). Acetals were converted to citral and citronellal during

and after complete conversion of citral. No nerol formation was observed. The quantities of other valuable products (geraniol and citronellol) were also low.

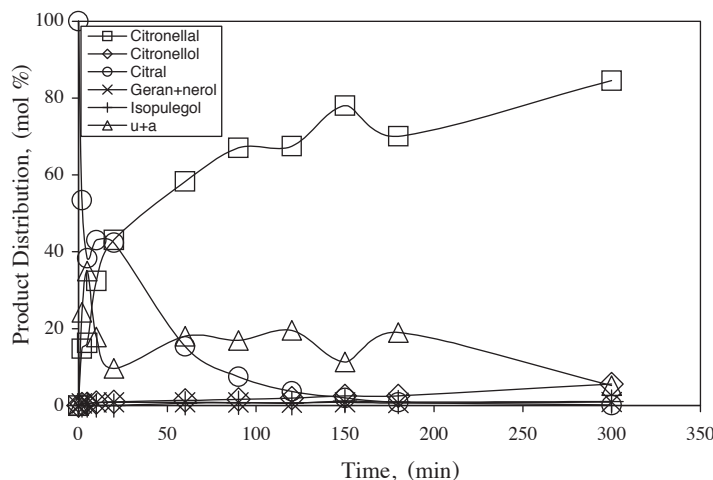


**Figure 4.** Product distribution obtained over Ni/Na-Y. u+a: unidentified+acetals.

The results of the reaction runs were analyzed in terms of yield and initial reaction rate:

$$Y_j = \text{yield of product } j = \frac{\text{moles of } j \text{ produced}}{\text{initial moles of citral}}$$

Yields of citronellal ( $Y_{cal}$ ) and acetal+unidentified products ( $Y_{u+a}$ ) over monometallic catalysts are given in Figure 5. As can be seen, citronellal was the major product over all the catalysts, and it increased in quantity over time. This shows that the conjugated bond of citral, not the carbonyl bond, was preferentially hydrogenated. The maximum yield of citronellal ranged between 73.2% and 84.5% over the monometallic catalysts. Acetals were formed at the beginning of the reaction. Once citral was almost completely converted, acetals were converted to citronellal. Citronellal acetal formation was the most abundant over Ni/Na-Mor, which had the highest concentration of acid sites.

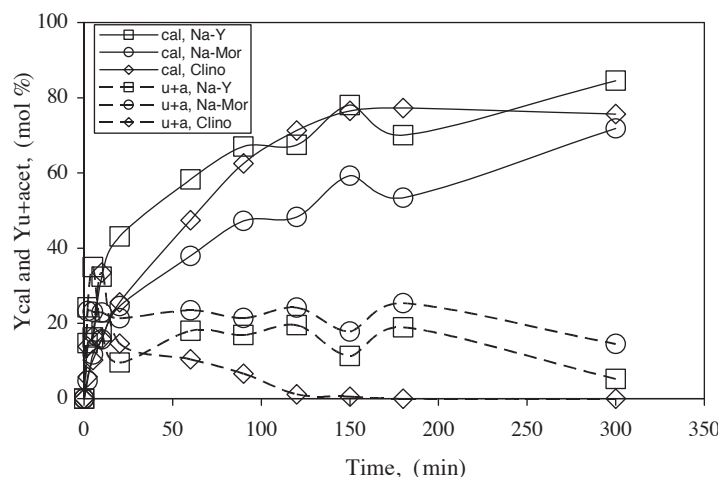


**Figure 5.**  $Y_{cal}$  and  $Y_{u+a}$  over monometallic catalysts.; cal: citronellal; u+a: unidentified+acetals.

The yield of geraniol+nerol ( $Y_{g+n}$ ) and citronellol ( $Y_{col}$ ) obtained over these catalysts are given in Figure 6.  $Y_{g+n}$  was low. The highest  $Y_{g+n}$  (5.5%) was obtained over Ni-Clino. There was no formation of

geraniol. Nerol was mainly formed at the beginning of the reaction and was then converted to citronellol. In contrast, there was no formation of nerol over Ni/Na-Y or Ni/Na-Mor, but geraniol did form at the beginning of the reaction and then increased slightly to  $Y_{g+n}$  of 0.9%.

$Y_{col}$  increased with reaction time and occurred in the following order: Ni/Clino (9.5%) > Ni/Na-Y (5.6%) > Ni-Mor (2.3%). These results show that Ni catalysts were more selective to citronellol at longer reaction times. Progress of the reactions showed that as the reaction continued over time citronellal was converted to citronellol.

Ni-supported catalysts have been reported to be selective to citronellol. Arvela et al. reported that Ni/Al<sub>2</sub>O<sub>3</sub> and Ni/SiO<sub>2</sub> gave high selectivity to citronellol (> 70%).<sup>5</sup> Usually less than 2% nerol and geraniol were formed, but H and NH<sub>4</sub> forms of the Y zeolite-supported Ni gave undesired products. This was attributed to the presence of strong acid sites. The importance of the Y zeolite form was also shown in a study by Blackmond et al.<sup>14</sup> Additionally, the preparation method can result in differences in product distribution. Very high selectivities for citronellol (above 90%) were obtained over a commercial Ni/Al<sub>2</sub>O<sub>3</sub> catalyst and over a fibrous Ni/SiO<sub>2</sub> catalyst.<sup>4</sup> Yilmaz et al. reported that a Pd/Clino catalyst gave citronellal with selectivity > 90%.<sup>10</sup>

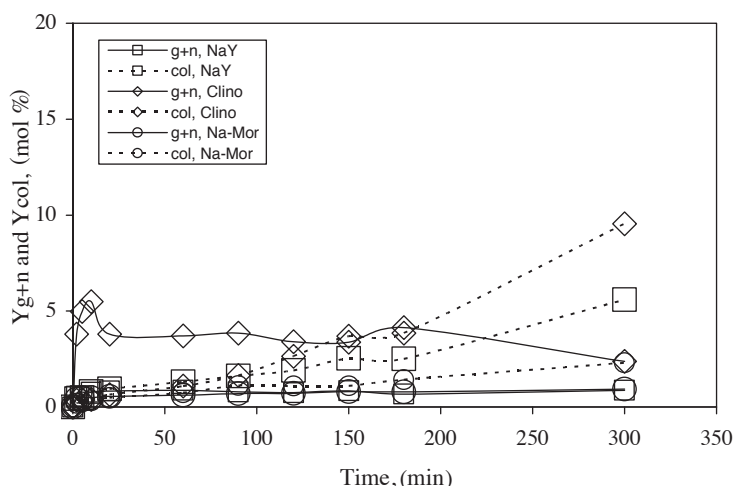


**Figure 6.**  $Y_{g+n}$  and  $Y_{col}$  over monometallic catalysts.; col: citronellol; g+n: geraniol+nerol.

The yields of citronellal and acetals over bimetallic Ni-Sn catalysts are shown in Figure 7. The major product was, again, citronellal. Both catalysts showed similar  $Y_{cal}$ ; the highest  $Y_{cal}$  was 44.5% over Ni-Sn/Na-Y and 42.0% over Ni-Sn/Na-Mor. Yields of citronellal over bimetallic catalysts were lower than those of monometallic catalysts. Significant acetal formation was observed. More acetal was formed over Ni-Sn/Na-Mor, as was the case with the monometallic catalysts. This catalyst had a higher concentration of acid sites than Ni-Sn/Na-Y.

Acetalization is an acid-catalyzed reaction. Acetalization could be due to support acidity, solvent acidity, or to use of a chloride-containing precursor.<sup>17</sup> Additionally, intra-zeolitic protons in zeolite and oxidized metal species on the catalyst have been reported to produce acetalization.<sup>9</sup> When the influence of the Lewis acidity effect is considered, findings differ. In one study an increase in Lewis acidity was reported to be beneficial for inhibiting acetalization,<sup>9</sup> while it was reported to increase acetalization in another study;<sup>18</sup> therefore, more research is needed in this respect. Acetal formation over bimetallic catalysts was similar in magnitude to that over monometallic catalysts, although the acidity of the bimetallic catalysts was lower

compared to their monometallic counter parts. Thus, the acetalization we observed was not primarily due to the acidity of the catalysts.

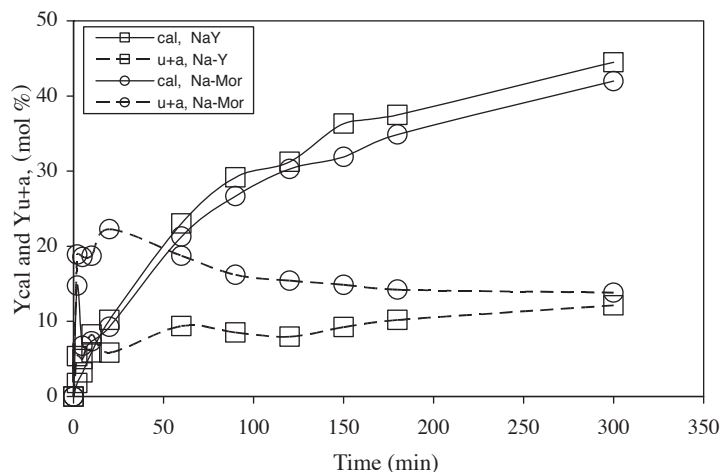


**Figure 7.**  $Y_{cal}$  and  $Y_{u+a}$  over bimetallic catalysts.; cal: citronellal; u+a: unidentified+acetals.

Figure 8 shows  $Y_{g+n}$  and  $Y_{col}$  obtained over bimetallic catalysts. Loading Sn to Ni catalysts increased the quantity of geraniol+nerol formed, and the increase was significant over Ni-Sn/Na-Mor;  $Y_{g+n}$  ranged from 0.9% to 6.3% over Ni-Sn/Na-Mor and from 0.9% to 2.1% over Ni-Sn/Na-Y. Formation of citronellol decreased significantly. This shows that the addition of Sn modified the catalyst in such a way that it improved carbonyl bond hydrogenation. This is in agreement with published findings that unsaturated alcohol formation increases with the addition of Sn to monometallic catalysts.<sup>5,7,10-14</sup> The increase in unsaturated alcohol was attributed to the higher concentration of weak acid sites and lower TPR temperature of Ni-Sn/Na-Mor (intimate contact) compared to Ni-Sn/Na-Y.

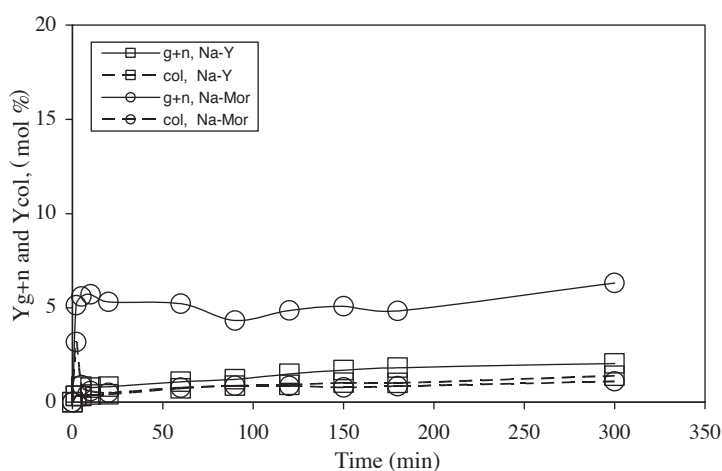


**Figure 8.**  $Y_{g+n}$  and  $Y_{col}$  obtained over bimetallic catalysts.; col: citronellol; g+n: geraniol+nerol.

Overall conversion ( $X$ ) and initial reaction rates ( $-r_0$ ) calculated for the different catalysts are given in Table 2. Very high conversion was obtained over the monometallic catalysts. Ni/Na-Y showed greater activity than the other monometallic catalysts, which had similar activity. Addition of Sn significantly

decreased the overall activity achieved over Ni-Sn/Na-Y, while it remained almost constant over Ni-Sn/Na-Mor. This difference could be attributed to different metal support interactions, as was shown by TPD and TPR results. Ni-Sn/Na-Mor had lower T<sub>max</sub> for H<sub>2</sub> desorption and was reduced with greater ease than Ni-Sn/Na-Y. These differences and differences in acidity gave the activities and product distributions obtained.

**Table 2.** Activity and yield of the different products over Ni and Ni-Sn catalysts.

	Ni/Na-Y	Ni/Clino	Ni/Na-Mor	Ni-Sn/Na-Y	Ni-Sn/Na-Mor
X	99.9	95.5	94.9	72.4	68.1
$-r_o$ , mmol/s of $g_{Ni}$	1.95	1.22	1.38	0.41	1.3

Initial rates obtained were comparable to those in the literature. In a study by Sordelli et al.,<sup>13</sup> addition of tin decreased catalytic activity with a corresponding increase in selectivity to unsaturated alcohols. It was concluded that the production of unsaturated alcohols needs an initial induction period during which the conjugated double bond is predominantly attached. Once unsaturated alcohols begin to form, the conjugated C=C bond hydrogenation rate rapidly decreases with time. This was suggested to be due to the coverage of active sites by Sn particulates.

## Conclusions

Product distribution was affected by the type of support material. Citronellal was the major product. After complete conversion of citral, citronellal was converted to citronellol. The Ni catalyst was selective to citronellal and citronellol. Addition of Sn increased geraniol and nerol formation, and suppressed citronellol formation. Activity of the catalysts was affected differently by different support types; it significantly decreased over Ni-Sn/Na-Y, while it remained constant over Ni-Sn/Na-Mor. This was attributed to differences in the interaction of Sn with different supports and active metals, as well as the acidity of the catalysts.

## Acknowledgments

The financial support provided by İzmir Institute of Technology Research Funds (BAP project, 2002-İYTE-14) is gratefully acknowledged.

## References

1. T. Salmi, P. Mäki-Arvela, E. Toukoniitty, A.K. Neyestanaki, L.P. Tiainen, L.E. Lindfors, R. Sjöholm and E. Laine, **Appl. Catal. A: Gen.** **196**, 93-102 (2000).
2. I.M.J. Vilella, S.R. de Miguel, de C.S.M Lecea, Á. Linares-Solano and O.A. Scelza, **Appl. Catal. A: Gen.** **281**, 247-258 (2004).
3. M.A. Aramendia, V. Borau, C. Jimenez, J.M. Marinas, A. Porras, and F.J. Urbano, **J. Catal.** **172**, 46-54 (1997).

4. A.M. Silva, O.A.A. Santos, M.J. Mendes, E. Jordão, and M.A. Fraga, **Appl. Catal. A: Gen.** **241**, 155-165 (2003).
5. P. Mäki-Arvela, L. Tiainen, M. Lindblad, K. Demirkan, N. Kumar, R. Sjöholm, T. Ollonqvist, J. Väyrynen, T. Salmi and D.Yu. Murzin, **Appl. Catal. A: Gen.** **241**, 271-288 (2003).
6. A.B. Da Silva, E. Jordao, M.J. Mendes and P. Fouilloux, **Appl. Catal. A: Gen.** **148**, 253 (1997).
7. J.N. Coupé, E. Jordão, M.A. Fraga and M.J. Mendes, **Appl. Catal. A: Gen.** **199**, 45-51, (2000).
8. A.P Jansen and R.A. van Santen, **J. Phys. Chem.** **94**, 6764 (1990).
9. S. Recchia, C. Dossi, A. Fusi, L. Sordelli and R. Psaro, **Appl. Catal. A: Gen.** **182**, 41-51 (1999).
10. S. Yılmaz, Ş. Ucar, L. Artok and H. Güleç, **Appl. Catal. A: General** **287**, 261-266 (2005).
11. P. Reyes, H. Rojas, G. Pecchi and J.L.G. Fierro, **J. Mol. Cat. A: Chem.** **179**, 293-299 (2002).
12. B. Baeza, I. Rodríguez-Ramos and A. Guerrero-Ruiz, **Appl. Catal. A: Gen.** **205**, 227-237 (2001).
13. L. Sordelli, R. Psaro, G. Vlaic, A. Cepparo, S. Recchia, C. Dossi, F. Achille and Z. Robertino, **J. Catal.** **182**, 186-198 (1999).
14. G. Blackmond, I.R. Oukaci, B. Blanc and P. Gallezot, **J. Catal.** **131**, 401-411 (1991).
15. A. Romero, A. Garrido, A. Nieto-Marquez, P. Sanchez, A. de Lucas, J.L. Valverde, **Micropor. Mesopor. Mater.** **110**, 318-329, 2008.
16. B. Bachiller-Baeza, A. Guerrero-Ruiz, P. Wang, I. Rodrigues-Ramos, **J. Catal.** **204**, 450-459, 2001.
17. J. Aumo, J. Lilja, P. Maki Arvela, T. Salmi, M. Sundell, H. Vainio, D. Yu Murzin, **Catal. Lett.** **84**, 219-224, 2002.
18. P. Maki-Arvela, L.P. Tianien, A.K. Neyestanaki, R. Sjöholm, T.K. Rantakyla, E. Laine, T. Salmi, D.Yu Murzin, **App. Catal. A: Gen** **237**, 181-200, 2002.

The printed version contains mistakes in the figures. The correct figures can be found below.

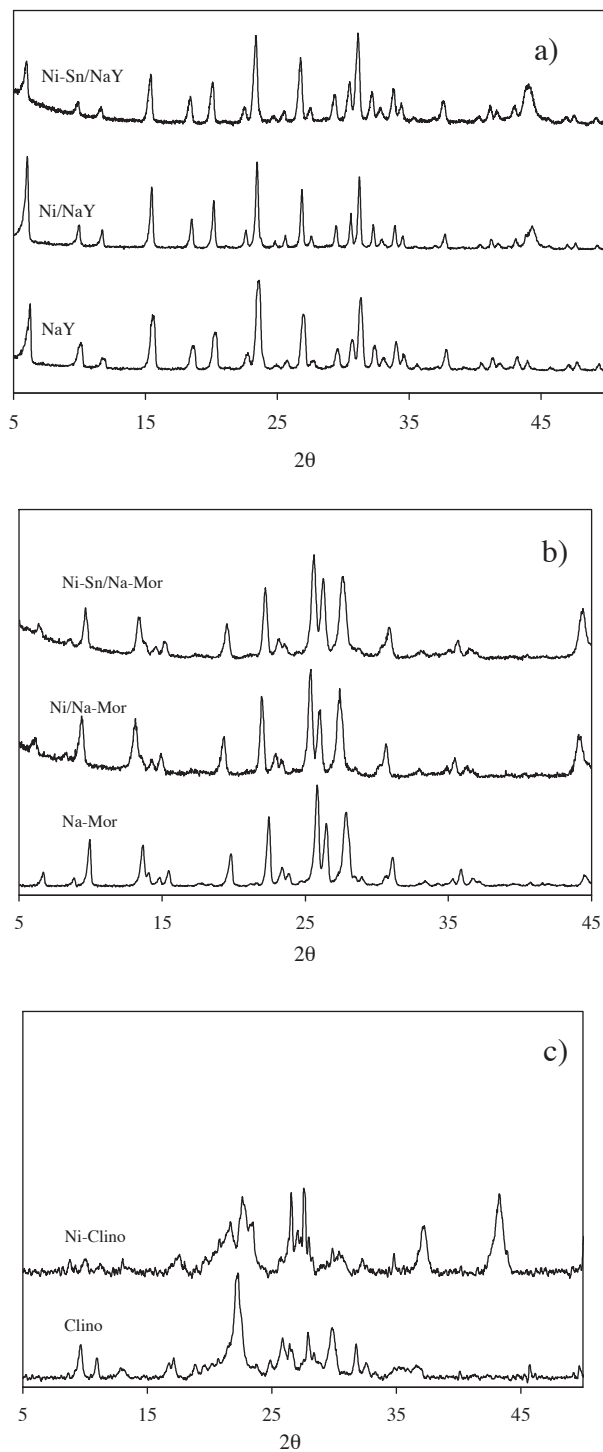


**Figure 2.** XRD patterns of the different supports and catalysts.; a) Na-Y and Na-Y-supported catalysts; b) Na-Mor and Na-Mor-supported catalysts; c) Clino and Clino-supported catalysts.

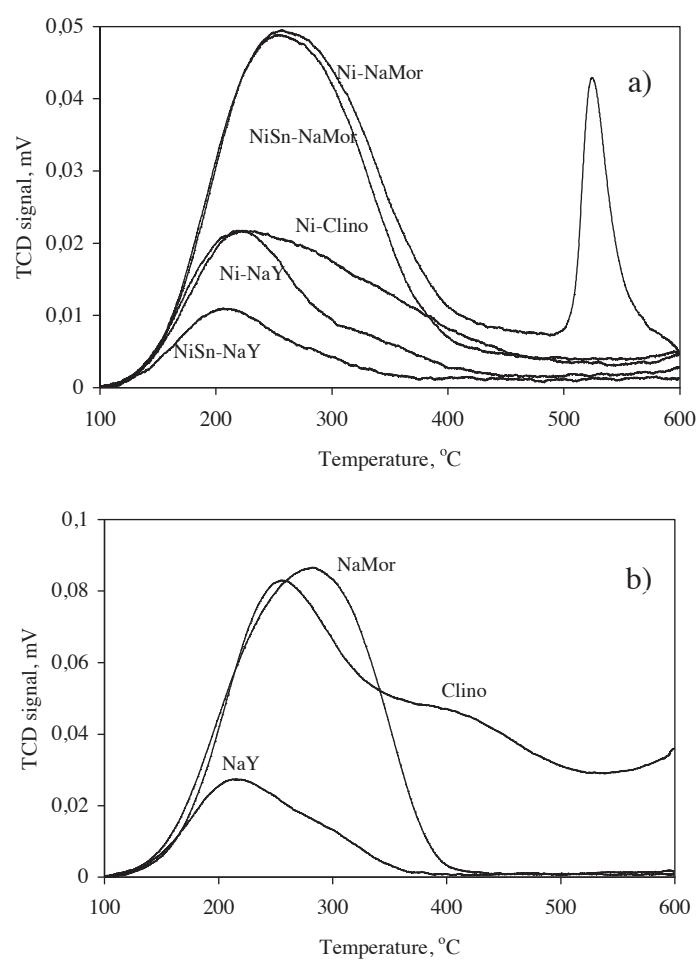


**Figure 3.** NH<sub>3</sub>-TPD of the catalysts (a) and the supports (b).